# Combined Cyclic Flexural-Torsional Loading Test of RC Columns

Paiboon Tirasit* and Kazuhiko Kawashima**

* M. of Eng., Graduate Student, Dept. of Civil Eng., Tokyo Institute of Technology, O-okayama, Meguro-ku, Tokyo 152-8552
** Dr. of Eng., Professor, Dept. of Civil Eng., Tokyo Institute of Technology, O-okayama, Meguro-ku, Tokyo 152-8552

Torsion probably takes place in the piers of some specific bridges during an earthquake and affects the pier seismic performance. This paper presents an experimental study on the inelastic behavior of reinforced concrete columns under combined action of cyclic bending and torsional loading. Seven reinforced concrete columns were tested under three loading conditions: 1) cyclic uniaxial bending; 2) cyclic torsion; and 3) combined cyclic bending and cyclic torsion, with and without a constant axial compression force. A parameter called "rotation-drift ratio" ($r$) was introduced to represent the level of combined cyclic bending and torsion. The experimental result indicates that the flexural capacity of reinforced concrete column decreases and the damage tends to occur above the flexural plastic hinge region as the rotation-drift ratio $r$ increases.

*Key Words: Torsion, bridge piers, seismic design, seismic performance*

## 1. Introduction

Presently, because of the space limitation for the transportation system in many urban areas, bridges with particular configurations, such as C-bent column bridges, skewed bridges and curved bridges, are often used. Due to their irregular structural configurations, the special seismic consideration is required to design these bridges to be able to survive extreme ground motions. Since the center of mass of superstructure does not coincide with the center of rigidity in C-bent columns, torsion coupled with other internal forces can occur during an earthquake. In skewed bridges, the collision between bridge deck and abutments or adjacent spans possibly takes place during a ground excitation and it subsequently causes the deck rotation about the vertical axis[1]. This may induce the twisting moment in the piers[2]. Moreover, the responses of curved bridges in the transverse and longitudinal directions are coupled, and the piers are subsequently subjected to the multi-directional deformation with torsion. The combination of seismic torsion and other internal forces can result in the complex flexural and shear failure of these bridge piers.

Although there have been a number of researches about the effect of twisting moment on the behavior of reinforced concrete member, most of them have focused on the monotonic load test. However, Hsu et al.[3] and Hsu et al.[4] conducted the experimental studies on the effect of combined cyclic bending and constant torsion on the performance of composite columns with H steel sections and hollow composite columns. They found that the flexural capacity and ductility of composite columns decreased when a constant torsion was simultaneously applied. The effect of torsion on the deterioration of flexural strength was more considerable in the composite columns with larger aspect ratio. Kawashima et al.[5] and Nagata et al.[6] conducted a cyclic bilateral loading test and a hybrid loading test, respectively, on the reinforced concrete C-bent columns. They revealed that the damage occurred severely on the eccentric compression side and the residual displacement happened in this direction. This was resulted from the eccentricity of vertical axial load cooperated with the bending moment and torsion form the eccentric lateral force. Otsuka et al.[7] carried out an experimental study on the performance of reinforced concrete columns under cyclic torsional loading. Their results indicated that the increase of axial force and amount of tie reinforcement enhanced the torsional capacity. Axial force and amount of tie bars affected the secondary stiffness of torsional hysteretic envelope. Otsuka et al.[8] also conducted a cyclic loading test on the reinforced concrete columns by applying a combined cyclic bending and torsion at each loading step. They found that the spacing of tie reinforcement remarkably affected the torsional hysteretic loops but less significantly influenced on flexural hysteretic loops.

However, there exist many unknowns on the effect of combined action of cyclic bending and torsion on the performance of reinforced concrete columns. Furthermore, the reliable torsional hysteretic model for the response analysis has not yet been available.

This paper presents a series of cyclic loading test of reinforced concrete columns to investigate the effect of combined cyclic bending and torsional loading on the column behavior. The experimental results about the progress of column failure, damage patterns and the hystereses are discussed.

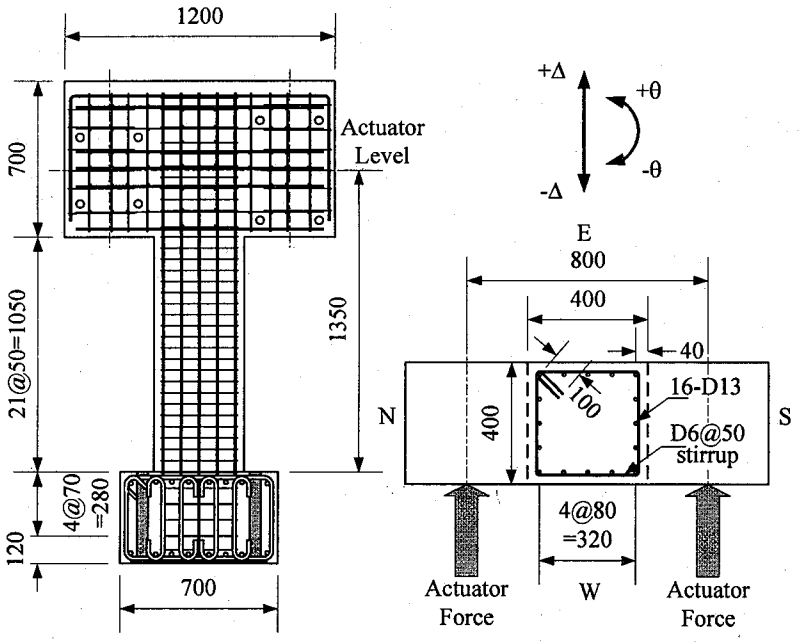


Fig. 1 Specimen configuration

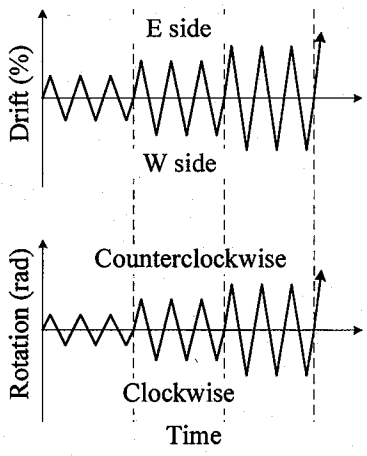


Fig. 2 Loading scheme

Table 1 Experimental cases

| Column | $f'_c$(MPa) | Loading scheme | $r$ |
|---|---|---|---|
| P1 | 28.6 | M+P | 0 |
| P2 | 28.3 | T | ∞ |
| P3 | - | T+P | ∞ |
| P4 | 32.2 | T+M+P | 0.5 |
| P5 | - | T+M+P | 1 |
| P6 | 32.8 | T+M+P | 2 |
| P7 | 33.1 | T+M+P | 4 |

T: Cyclic torsion, M: Cyclic uniaxial bending and P: 160kN constant axial compression force

## 2. Experimental Program

### 2.1 Properties of specimens

Seven reinforced concrete columns were constructed with the same structural properties as shown in Fig. 1. The column cross section was 400 mm x 400 mm square. The column was 1750 mm tall with a 1350 mm effective height measured from the bottom of column to the loading point. The columns were designed based on the Japanese 1996 Design Specifications for Highway Bridges[9]. Type I (middle-field) and Type II (near-field) ground motions with the moderate soil condition were assumed. The axial compression stress at the flexural plastic hinge region of the columns due to the superstructure dead weight was assumed to be 1 MPa which is typical in Japanese bridge piers. Sixteen 13mm diameter deformed bars with a 295 MPa nominal strength (SD295A) were employed as the longitudinal reinforcement. The same class 6mm deformed bars were used as the tie reinforcement with 50 mm spacing along the column axis. The tie bars were anchored using 135 degree bent hooks with a development length of 100 mm. The yield strengths of longitudinal and tie reinforcements were 353.7 MPa and 328 MPa, respectively. The longitudinal reinforcement ratio and the tie volumetric ratio were 1.27% and 0.75%, respectively. The design compressive strength of concrete was 30 MPa. Table 1 shows the concrete strength $f'_c$ obtained from the cylinder test. Because cylinder test was not conducted for P3 and P5, measured strength of concrete is not available. However, because the concrete was mixed and casted in the same way with other specimens, the concrete strength must be very similar with others. It is noted that these material properties and amount of reinforcements correspond to those of piers in typical bridges.

### 2.2 Test setup and loading

A series of cyclic loading test was conducted by employing the dynamic loading facility in Tokyo Institute of Technology. One vertical and two horizontal actuators were used to conduct the test. A constant 160 kN compression load was applied to the columns by the vertical actuator in order to produce a 1 MPa compressive stress in the flexural plastic hinge region. The column surfaces are designated here as N, W, S and E as shown in Fig. 1. To apply cyclic uniaxial bending, cyclic torsion and combined cyclic uniaxial bending and torsion to the columns, lateral displacement and rotation were generated by controlling two horizontal actuators as shown in Fig. 1. Cyclic uniaxial bending was created by driving two horizontal actuators with the same displacement commands while cyclic torsion and combined cyclic uniaxial bending and torsion were generated by imposing different displacement commands in two actuators.

A non-dimensional parameter called "rotation-drift ratio", $r$, is introduced here to define the level of combined cyclic bending and torsion as

$$r = \frac{\theta}{\Delta} \tag{1}$$

Table 2 Applied lateral drifts and rotations of each loading step

| Loading step | P1 ($r$=0) | P2 ($r$=∞) | P3 ($r$=∞) | P4 ($r$=0.5) | | P5 ($r$=1) | | P6 ($r$=2) | | P7 ($r$=4) | |
|---|---|---|---|---|---|---|---|---|---|---|---|
| | Drift Δ(%) | θ (rad) | θ (rad) | θ (rad) | Drift Δ(%) | θ (rad) | Drift Δ(%) | θ (rad) | Drift Δ(%) | θ (rad) | Drift Δ(%) |
| 1 | 0.25 | 0.0025 | 0.0025 | 0.00125 | 0.25 | 0.0025 | 0.25 | 0.0025 | 0.125 | 0.0025 | 0.0625 |
| 2 | 0.5 | 0.005 | 0.005 | 0.0025 | 0.5 | 0.005 | 0.5 | 0.005 | 0.25 | 0.005 | 0.125 |
| 3 | 1 | 0.01 | 0.01 | 0.005 | 1 | 0.01 | 1 | 0.01 | 0.5 | 0.01 | 0.25 |
| 4 | 1.5 | 0.02 | 0.02 | 0.0075 | 1.5 | 0.015 | 1.5 | 0.02 | 1 | 0.02 | 0.5 |
| 5 | 2 | 0.03 | 0.03 | 0.01 | 2 | 0.02 | 2 | 0.03 | 1.5 | 0.03 | 0.75 |
| 6 | 2.5 | 0.04 | 0.04 | 0.0125 | 2.5 | 0.025 | 2.5 | 0.04 | 2 | 0.04 | 1 |
| 7 | 3 | 0.05 | 0.05 | 0.015 | 3 | 0.03 | 3 | 0.05 | 2.5 | 0.05 | 1.25 |
| 8 | 3.5 | 0.06 | 0.06 | 0.0175 | 3.5 | 0.035 | 3.5 | 0.06 | 3 | 0.06 | 1.5 |
| 9 | 4 | 0.07 | 0.07 | 0.02 | 4 | 0.04 | 4 | - | - | 0.07 | 1.75 |
| 10 | 4.5 | 0.08 | 0.08 | 0.0225 | 4.5 | - | - | - | - | 0.08 | 2 |
| 11 | 5 | 0.09 | 0.09 | 0.025 | 5 | - | - | - | - | 0.09 | 2.25 |
| 12 | - | - | 0.1 | - | - | - | - | - | - | - | - |

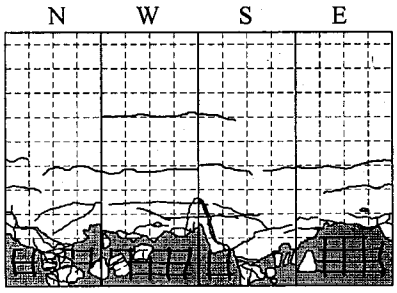


(a) Damage after loading (5% drift)

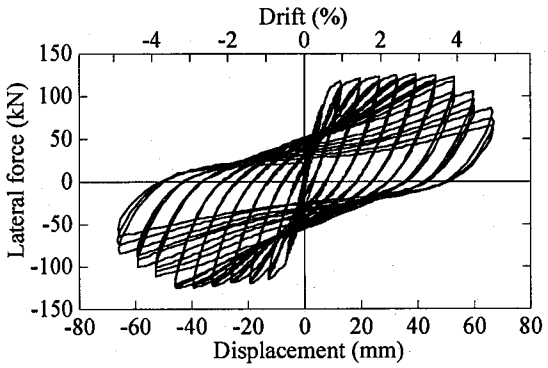


(b) Flexural hysteresis

Fig. 3 Damage after testing and flexural hysteresis of column P1 (cyclic uniaxial bending with an axial force)

where $\theta$ is the column rotation (radian) and $\Delta$ is the lateral drift of column which is the ratio of the column lateral displacement and the effective height. $\Delta$ is represented in % herein after.

The rotation-drift ratios $r$ and the applied lateral drifts and rotations of every loading step of all columns are presented in Table 2. P1 was tested under cyclic uniaxial bending. To investigate the effect of axial force on the torsional hysteresis of column, P2 and P3 were tested under pure cyclic torsion without and with an axial compression force, respectively. Results from P1 and P3 were used as the references of this study. P4 to P7 were loaded under several combinations of cyclic bending and torsion which were represented by the rotation-drift ratio $r$ defined by Eq. (1). The lateral drift and rotation were simultaneously applied three cycles at every loading step as shown in Fig. 2. According to Figs. 1 and 2, because the positive directions of the lateral displacement and the rotation were in the east and counterclockwise directions respectively, and vice versa, the S surface suffered larger deformation than the N surface in the columns under combined cyclic bending and torsion. This affected the behavior of columns as explained later in the next section.

## 3. Damage and Hystereses of Columns

### 3.1 Column under cyclic uniaxial bending

Fig. 3(a) presents the damage at the completion of loading at 5% drift of P1 which was subjected to cyclic uniaxial bending with the axial force. The covering concrete on E surface in the plastic hinge region firstly suffered the compression failure at 3% drift. Consequently, the spalling off began to take place in the covering concrete and the longitudinal and tie reinforcements were uncovered at 4% drift. After that some longitudinal reinforcement buckled at 4.5% drift at 0 to 200 mm high from the base of column and the damage continuously developed.

The flexural hysteresis of P1 is shown in Fig. 3(b). The column flexural restoring force is virtually stable between 1% to 4% drift with the flexural strength of 125.9 kN. The flexural restoring force starts to deteriorate at 3% drift because of the occurrence of compression failure in the covering concrete and the buckling of longitudinal reinforcement. Subsequently, the column looses the lateral confinement, and the flexural restoring force deteriorates to 68.7% of the flexural strength at 5% drift.

### 3.2 Columns under cyclic torsion

Diagonal cracks first initiated at 0.005 radian rotation cycle in P3 which was subjected to cyclic torsion with the axial force. Subsequently, the number of cracks increased and checker board crack patterns were formed on all column surfaces. Then the crack widths enlarged and the covering concrete spalled outward as the applied rotation increased. The damage of P3 at the completion of

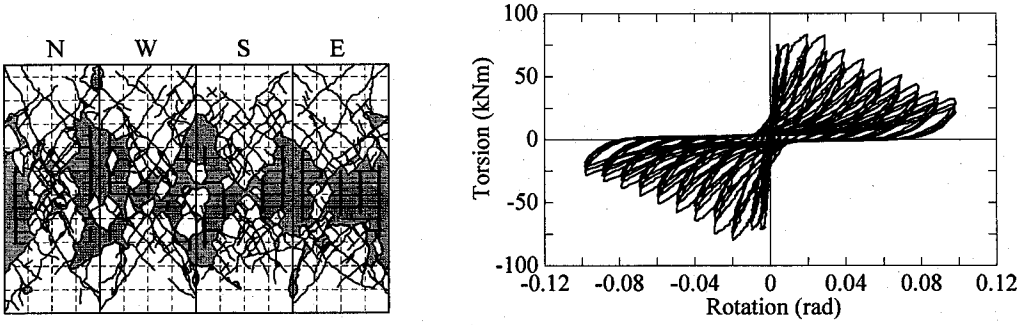


(a) Damage after loading (0.1 rad) (b) Torsional hysteresis

Fig. 4 Damage after testing and torsional hysteresis of column P3 (cyclic torsion with an axial force)

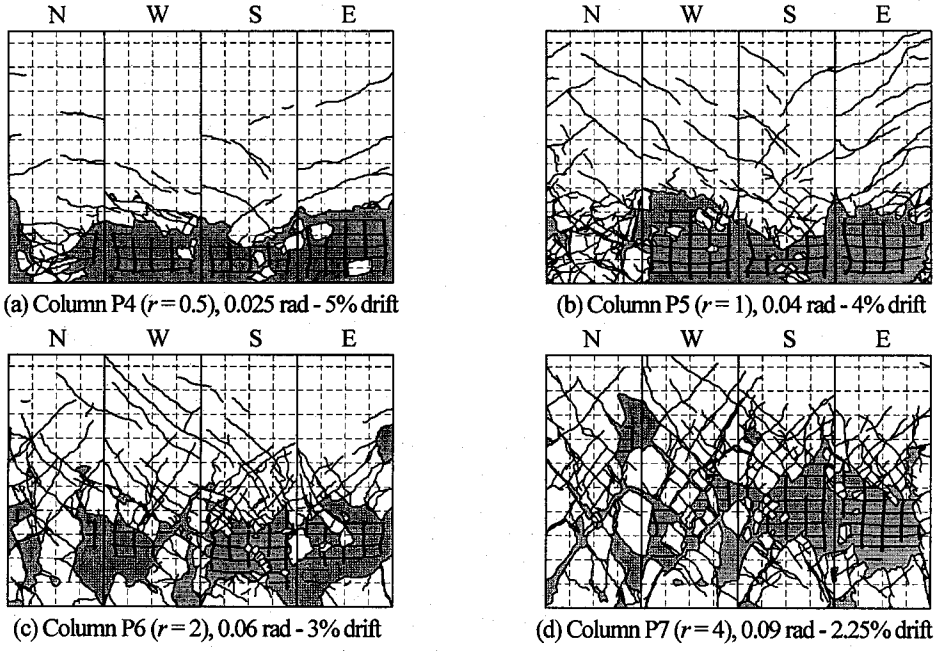


(a) Column P4 ($r$ = 0.5), 0.025 rad - 5% drift (b) Column P5 ($r$ = 1), 0.04 rad - 4% drift

(c) Column P6 ($r$ = 2), 0.06 rad - 3% drift (d) Column P7 ($r$ = 4), 0.09 rad - 2.25% drift

Fig. 5 Damage after testing of columns P4 to P7 (combined cyclic uniaxial bending-torsional loading)

loading is presented in Fig. 4(a). The significant damage took place at the column mid height and the longitudinal bars slightly buckled outward. The damage patterns of this column are considerably different to that of P1 under cyclic bending. Substantial damage occurred at the middle of column instead of the typical flexural plastic hinge zone which is generally about a half of the column width from the base of column.

Fig. 4(b) shows the torsional hysteresis of P3. The torsional stiffness sharply deteriorates after cracking at 0.005 radian rotation cycle. Then P3 reaches the torsional strength of 83.4 kNm at 0.02 radian and it is followed by rather sharp deterioration due to the damage progress at the middle of column. As a consequence, the torsional capacity of P3 deteriorates to 76.3% of its strength at 0.05 radian.

### 3.3 Columns under combined cyclic uniaxial bending and torsion

Behavior of columns subjected to combined cyclic bending and torsion was investigated under four different rotation-drift ratios $r$. The damage at the end of loading on P4 to P7 is shown in Fig. 5. It can be seen that the S surface suffered more significant damage than the N surface. This was because the loading displacement resulted from combined bending and torsion was larger at the S surface than the N surface as explained in section 2.2. Moreover, the angles of cracks relative to the column cross section increased as $r$ increased. Compared to the damage of P1 subjected to cyclic bending in Fig. 3(a), more complex flexural and shear failure took place and the damage occurred above the plastic hinge region as $r$ increased. The damage pattern of P4 with $r = 0.5$ was not so far different from that of P1 subjected to pure cyclic bending.

Fig. 6 shows the flexural and torsional hystereses of P4 to P7. It can be observed that the flexural hystereses of P5 to P7 are significantly different to the flexural hysteresis of P1 under cyclic bending shown in Fig. 3(b). Furthermore, the torsional hystereses of P4 to P6 are considerably different to the torsional hysteresis of P3 under cyclic torsion as shown in Fig. 4(b). In addition, it can be clearly seen that the flexural strength and the flexural ductility of columns decrease as $r$ increases. On the other hand, the torsional strength and the torsional ductility decrease as $r$ decreases.

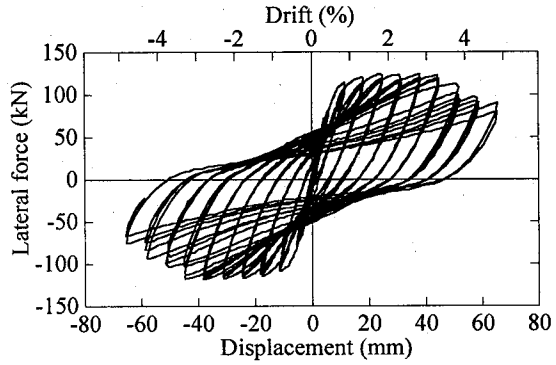


(a) Flexural hysteresis

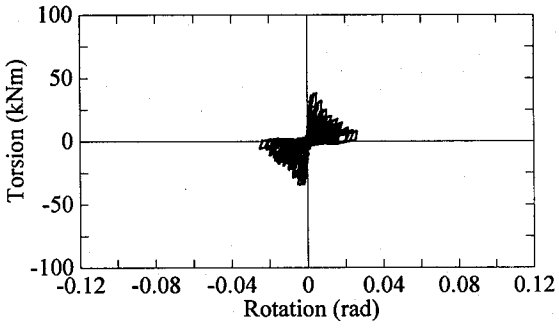


(b) Torsional hysteresis

(1) Column P4 ($r=0.5$)

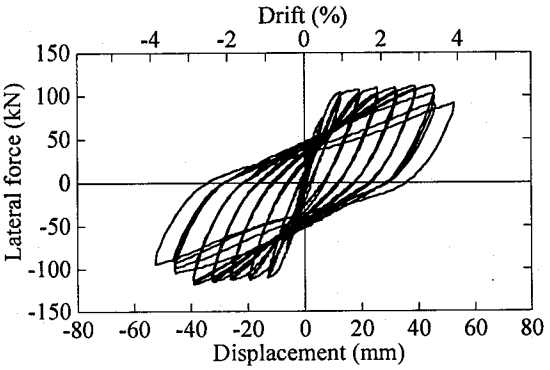


(a) Flexural hysteresis

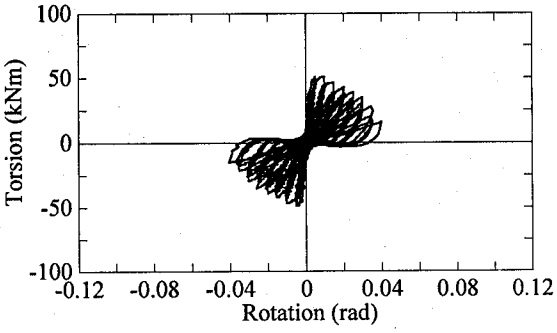


(b) Torsional hysteresis

(2) Column P5 ($r=1$)

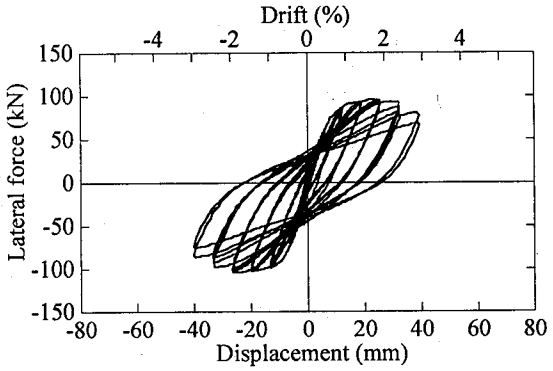


(a) Flexural hysteresis

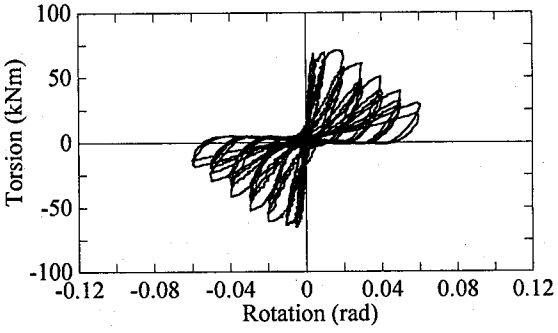


(b) Torsional hysteresis

(3) Column P6 ($r=2$)

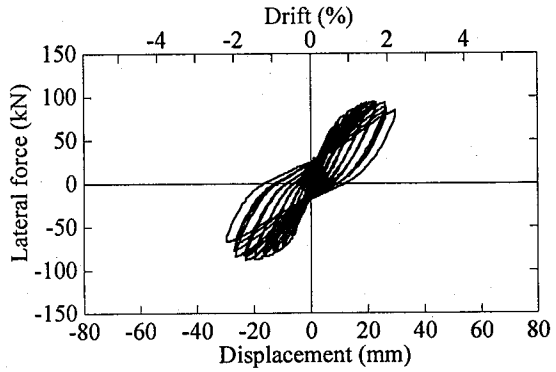


(a) Flexural hysteresis

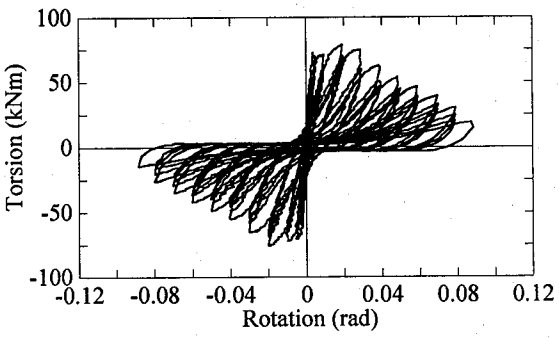


(b) Torsional hysteresis

(4) Column P7 ($r=4$)

Fig. 6 Flexural and torsional hystereses of columns under combined cyclic bending-torsional loading

Table 3 Maximum lateral forces and torsions

| Column | $r$ | Maximum lateral force (kN) | | | Maximum torsion (kNm) | | |
|---|---|---|---|---|---|---|---|
| | | Positive | Negative | Average | Positive | Negative | Average |
| P1 | 0 | 125.9 | 125.2 | 125.6 (100%) | - | - | - |
| P2 | ∞ | - | - | - | 75.7 | 70.0 | 72.9 (89.3%) |
| P3 | ∞ | - | - | - | 83.4 | 79.7 | 81.6 (100%) |
| P4 | 0.5 | 124.2 | 118.5 | 121.4 (96.7%) | 38.4 | 34.7 | 36.6 (44.8%) |
| P5 | 1 | 111.5 | 117.9 | 114.7 (91.4%) | 50.8 | 48.4 | 49.6 (60.8%) |
| P6 | 2 | 95.9 | 103.8 | 99.9 (79.5%) | 71.0 | 64.9 | 68.0 (83.3%) |
| P7 | 4 | 94.4 | 88.0 | 91.2 (72.6%) | 79.0 | 75.6 | 77.3 (94.8%) |

Table 4 Ultimate displacements and rotations

| Column | $r$ | Ultimate displacement (% drift) | | | Ultimate rotation (rad) | | |
|---|---|---|---|---|---|---|---|
| | | Positive | Negative | Average | Positive | Negative | Average |
| P1 | 0 | 5 | 4.5 | 4.75 (100%) | - | - | - |
| P2 | ∞ | - | - | - | 0.05 | 0.05 | 0.05 (100%) |
| P3 | ∞ | - | - | - | 0.05 | 0.05 | 0.05 (100%) |
| P4 | 0.5 | 4.5 | 4.5 | 4.5 (94.7%) | 0.01 | 0.01 | 0.01 (20%) |
| P5 | 1 | 4 | 4 | 4 (84.2%) | 0.025 | 0.025 | 0.025 (50%) |
| P6 | 2 | 3 | 3 | 3 (63.2%) | 0.04 | 0.04 | 0.04 (80%) |
| P7 | 4 | 2.25 | 2.25 | 2.25 (47.4%) | 0.04 | 0.04 | 0.04 (80%) |

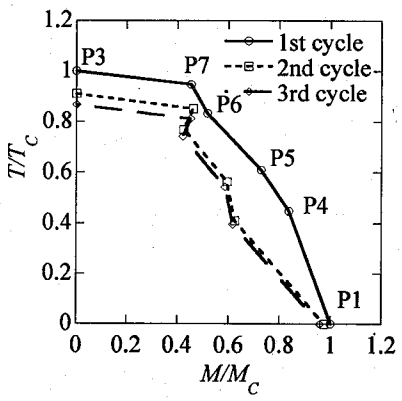


Fig. 7 Normalized interaction curves

## 4. Influence of Combined Cyclic Uniaxial Bending-Torsional Loading

### 4.1 Lateral force and torsional capacities, and ultimate displacement and rotation

The maximum lateral force and torsional capacities, and the ultimate displacement and rotation of seven columns are summarized in Tables 3 and 4, respectively. The ultimate displacement is defined here as the displacement where the lateral restoring force deteriorates to less than 80% of the flxerural strength and the ultimate rotation is defined as the rotation where the torsional restoring force degrades to less than 80% of the torsional capacity. The results of P1 under cyclic uniaxial bending and P3 under cyclic torsion with the axial force are used as the benchmarks to evaluate the deterioration of the flexural and torsional strengths and the ultimate displacement and rotation of the columns under combined action. It is apparent that the flexural strength and the ultimate displacement deteriorate as $r$ increases and the torsional strength and the ultimate rotation deteriorate as $r$ decreases. It is worthy to note that columns under combined action reached their maximum torsions prior to the maximum lateral forces in both positive and negative directions. Moreover, the columns reached the ultimate rotations before the ultimate displacements. At $r = 4$, the flexural strength and the ultimate displacement are 72.6% and 47.4% of the column under cyclic uniaxial bending, respectively. From P2 and P3, it is apparent that axial compression force enhances the torsional strength of column.

### 4.2 Normalized interaction curves

Fig. 7 shows the normalized interaction curves between bending moment and torsion obtained from the experimental results. The values of each point in the plot are based on the averages of the maximum torsion or maximum bending moment, depending on which value the column reached first, and the corresponding bending moment or torsion. The columns under combined cyclic bending and torsion reached their maximum torsions prior to the maximum bending moments as mentioned in section 4.1. Torsion $T$ of each column is normalized by the average maximum torsion $T_c$ in the first loading cycle of P3 under cyclic torsion and bending moment $M$ is normalized by the average maximum bending moment $M_c$ in the first loading cycle of P1 under cyclic bending. It can be seen that torsion deteriorates with the increase of bending moment, and vice versa. The effect of number of loading cycles can also be observed from the difference between the curves of the first and second loading cycles. However, less significant difference is seen between the curves of the second and third loading cycles. This indicates that the deterioration of column capacities is significant in the first loading cycle and tends to become less significant after columns undergo some more loading repetitions. It is noted that the effect of large number of loading cycles is out of consideration in this study.

## 5. Conclusions

An experimental study on the effect of combined cyclic uniaxial bending and torsion on the behavior of reinforced concrete columns was presented. Various combinations of bending and torsion in the form of the rotation-drift ratio $r$ were tested to clarify the column performance. Based on the results presented herein, it may be concluded that:

1) The existence of torsion alters the damage patterns of reinforced concrete columns under combined action. The complex flexural and shear failure tends to occur and the damage is likely to shift outside the typical flexural plastic hinge region to the middle of column as $r$ increases. Because the length and location of plastic hinge significantly change, they have to be carefully evaluated in the column under combined bending moment and torsion.
2) The flexural capacity and the ultimate displacement of column deteriorate as the torsion increases. In contrast, the increase of bending moment leads to the deterioration of the torsional capacity and the ultimate rotation. Consequently, it is necessary to take account of this interaction in design of column subjected to the combined flexural and torsional load.
3) The relationship between the internal bending moment and torsion of columns can be performed as the normalized interaction curves. Increase of the number of loading cycles results in the reduction of the area enclosed by the interaction curve.

## Acknowledgements

The authors express their sincere gratitude to Messrs. Watanabe, G., Fukuda, T., Nagai, T., Wang, Y., Ogimoto, H., Kijima, K., Nagata, S., Maruyama, Y. and Ms. Sakellaraki, D. for their extensive support in constructing the columns and executing the experiment.

## References

1) Watanabe, G. and Kawashima, K., Effectiveness of Cable-restrainer for Mitigating Rotation of a Skewed Bridge Subjected to Strong Ground Shaking, *13th World Conference on Earthquake Engineering*, Vancouver, Canada, Paper No. 789, 2004.
2) Tirasit, P. and Kawashima, K., Seismic Torsion Response of Skewed Bridge Piers, *Journal of Earthquake Engineering* 28, Paper No. 116, JSCE, 2005.
3) Hsu, H.-L. and Wang, C.-L., Flexural–Torsional Behavior of Steel Reinforced Concrete Members subjected to Repeated Loading, *Earthquake Engineering and Structural Dynamics* 29, 667–682, 2000.
4) Hsu, H.-L. and Liang, L.-L., Performance of Hollow Composite Members subjected to Cyclic Eccentric loading, *Earthquake Engineering and Structural Dynamics* 32, 433–461, 2003.
5) Kawashima, K., Watanabe, G., Hatada, S. and Hayakawa, R. Seismic Performance of C-bent Columns based on a Cyclic Loading Test, *Journal of Structural Mechanics and Earthquake Engineering* 745/I–65, pp.171–189, 2003 (In Japanese)
6) Nagata, S., Kawashima, K. and Watanabe, G., Seismic Performance of Reinforced Concrete C-bent Columns based on a Hybrid Loading Test, *Proc. of the First International Conference on Urban Earthquake Engineering*, Tokyo Institute of Technology, Tokyo, Japan, pp.409–416, 2004.
7) Otsuka, H., Wang, Y., Takata, T. and Yoshimura, T., Experimental Study on the Parameters Effecting the Hysteresis Loop of RC Members subjected to Pure Torsion, *Journal of Structural Mechanics and Earthquake Engineering* 739/V-60, pp.93–104, 2003 (In Japanese)
8) Otsuka, H., Takeshita, E., Yabuki, W., Wang, Y., Yoshimura, T. and Tsunomoto, M., Study on the Seismic Performance of Reinforced Concrete Columns subjected to Torsional Moment, Bending Moment and Axial Force, *13th World Conference on Earthquake Engineering*, Vancouver, Canada, Paper No. 393, 2004
9) Japan Road Association, *Specifications for Highway Bridges - Part V Seismic Design*, Maruzen, Tokyo, 1996.

(Received September 10, 2005)